New Analytical Model for Nanoscale Tri-Gate SOI MOSFETs Including Quantum Effects

P. Vimala, *Student Member, IEEE* and N. B. Balamurugan, *Member, IEEE*

***Abstract*—In this paper, an analytical model for tri-Gate (TG) MOSFETs considering quantum effects is presented. The proposed model is based on the analytical solution of Schrodinger–Poisson's equation using variational approach. An analytical expression of the inversion charge distribution function (ICDF) or wave function for the TG MOSFETs has been developed. This obtained ICDF is used to calculate the device parameters, such as the inversion charge centroid, threshold voltage, inversion charge, gate capacitance, and drain current. These parameters are modeled for various device dimensions and applied bias. The results are validated against the TCAD simulation results.**

***Index Terms*—Device modeling, energy quantization, inversion charge, Poisson–Schrodinger equation, tri-gate MOSFET.**

I. Introduction

THE CONTINUING downscaling of the conventional complementaryMOS (CMOS) has been hindered by the growing deleterious presence of the short-channel effects (SCEs) [1], [2]. As the semiconductor devices begin to enter the deep sub-micrometer regime, the short-channel effects (SCEs) phenomenon will take on a more prominent role in affecting their performance. Reducing the SCEs has become crucial for improving the capabilities of MOSFETs. Therefore, research on reducing the SCE is currently being carried out. In particular, attention is focused on multiple-gate MOSFETs because of their steep sub-threshold slope and low body-effect coefficient [3]–[7]. Among the various types of multiple-gate MOSFETs, Tri-Gate (TG) MOSFETs have attracted much attention for downscaling CMOS technology up to 10 nm channel length owing to its superior gate control over the channel and high current drive capability [8].

The effect of quantization of electronic energy becomes significant for 10 nm and thus it is extremely important to consider quantum effects in MOSFET models. Several classical models have been developed for triple-gate structure [9]–[11]. A complete model should also include the quantum effects [12]. Previously, the energy quantization has been analytically modeled for double-gate (DG) MOSFETs [13] and surrounding gate (SG) MOSFETs [14]. Some models have been established for analyzing quantum effects in Si trigate MOSFETs. The numerical simulations have been reported for quantum effects in trigate MOSFETs [15], [16]. Mathematical complexity of these models is not suitable for compact modeling. In order to simplify this problem a good analytical model has to be developed for solving the coupled Poisson and Schrodinger equations. The analytical quantum model for trigate MOSFET is [17] proposed the analytical solution of two-dimensional Poisson's-Schrodinger equation. But it is suitable for long channel devices and they account only the inversion charge and threshold voltage modeling. To the best of our knowledge, so far the complete analytical quantam modeling for trigate MOSFET has not been described.

Therefore, the purpose of this paper is to derive an accurate quantum analytical model for TG MOSFETs. The energy and wavefunction of the channel charge carriers are essential to model the quantum effect, and they can be determined by solving Schrodinger equation. Our model is based on the analytical solution of Poisson's-Schrodinger equation using variational approach. The variational technique represents a completely different way of getting approximate energies and wave functions for quantum mechanical systems.The technique involves guessing a reasonable, parametric form for a trial wave function ($\psi_0(x, y)$).

The rest of the paper is organized as follows: Section II presents the generation of quantum analytical model for trigate MOSFET. In Section III, the analytical models for important device parameters are extracted as a function of device dimensions and applied bias. Descriptions of main results are presented in Section IV. Finally the conclusions are given in Section V.

II. Quantum Modeling

The structure and schematic view of the trigate MOSFET cross section is shown in Fig. 1 with silicon width W, silicon thickness H and the gate oxide thickness Tox. For this structure, we solved the Poisson and Schrodinger equations using variational approach to obtain the quantum effects. These equations have to be solved consistently to obtain the electric potential distribution and energy levels. The Poisson equation for the trigate MOSFETs is given as,

$$\frac{d^2\phi(x, y)}{dx^2} + \frac{d^2\phi(x, y)}{dy^2} = -\frac{q}{\varepsilon_{si}} n(x, y) \tag{1}$$

Manuscript received September 19, 2013; revised December 20, 2013; accepted January 2, 2014. Date of publication January 9, 2014; date of current version February 12, 2014. This work was supported by the Women Scientist Scheme-A, Department of Science and Technology, New Delhi, Government of India, under Grant SR/WOS-A/ET-41/2011. The review of this paper was arranged by Editor R. Singh.

The authors are with the Department of Electronics and Communication Engineering, Thiagarajar College of Engineering, Tamil Nadu 625005, India (e-mail: vimalapalanichamy@tce.edu; nbbalamurugan@tce.edu).

Color versions of one or more of the figures in this paper are available online at http://ieeexplore.ieee.org.

Digital Object Identifier 10.1109/JEDS.2014.2298915

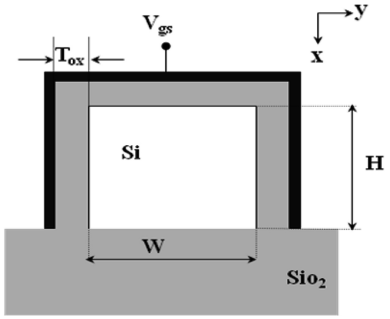

Fig. 1. Cross section of the silicon trigate MOSFETs under study.

where q is the electronic charge, ε_{si} is the silicon permittivity, $\phi(x, y)$ is the electric potential in the silicon, $n(x, y)$ is the electron density.

To include the quantum effects, the relation between the $n(x, y)$ and the trial wave function $\psi_0(x, y)$ is given as,

$$|\psi_0(x, y)|^2 = \frac{n(x, y)}{N_{inv}} \tag{2}$$

where N_{inv} is inversion charge density. Substituting (2) into (1), we can get,

$$\frac{d^2\phi(x, y)}{dx^2} + \frac{d^2\phi(x, y)}{dy^2} = -\frac{q}{\varepsilon_{si}} N_{inv} |\psi_0(x, y)|^2 \tag{3}$$

The Poisson equation for trigate MOSFETs quantum model is expressed in (3), according to the wave function $\psi_0(x, y)$.

The wave function is essential to study the quantum effects, and it can be determined by solving the Poisson and Schrodinger equations. Previously, we have proposed the trial wave function for double gate structure [13] and Moreno et al. [18] have introduced the trial wave function for square gate all around MOSFET. Using these two equations, we have proposed the optimum trial wavefunction for TG MOSFETs as,

$$\psi_o(x, y) = \begin{pmatrix} a_0\sqrt{4/HW}\sin\left(\frac{\pi x}{H}\right)\left[\sin\left(\frac{\pi y}{W}\right)\right]^{1/2}\exp\left(\frac{-b_0 x}{H}\right) \\ \left[\exp\left(\frac{-b_0 y}{W}\right) + \exp\left(\frac{-b_0(W-y)}{W}\right)\right] \end{pmatrix} \tag{4}$$

where a_0 is the normalization constant and b_0 is the variational parameter which will be determined later.

Normalization of (4) $\int_0^W \int_0^H |\psi_o(x, y)|^2\, dxdy = 1$ gives,

$$a_0 = \sqrt{\frac{b_0 HW(4b_0^4 + 5b_0^2\pi^2 + \pi^4)}{8\pi HW\sinh(b_0)\cosh(2b_0) + \sinh(2b_0)\begin{pmatrix} 4b_0^2 + \pi^2 \\ +\pi^2\cosh(b_0)\end{pmatrix}}} \tag{5}$$

Now we got the value of normalization constant in terms of b_0. In order to get the analytical solution of the Poission equation, integrating (3) twice from $x = 0$ to W and $y = 0$ to H. We can obtain the electric potential according to b_0 is given in (6).

where,

$\alpha = \frac{b_0(H+2y)}{H}$, $\beta = \frac{2b_0(H(W-x)+Wy)}{HW}$, $\gamma = \frac{2b_0(Hx+Wy)}{HW}$, $\omega = \pi^2H^2 + 4b_0^2W^2$ and $\delta = -4HW\pi^2 + 4\pi^2W$

The unknown parameter b_0 can be computed by solving the following Schrodinger equation

$$\left(\frac{\hbar^2}{2m_x}\frac{d^2\psi_0(x, y)}{dx^2} + \frac{\hbar^2}{2m_y}\frac{d^2\psi_0(x, y)}{dy^2} - q\phi\psi_0(x, y)\right) = E_0\psi_0(x, y) \tag{7}$$

Here $\hbar = h/(2\pi)$, his the Planck's constant, $m_x = 0.916m_0$ and $m_y = 0.190m_0$ are the effective masses of electrons along x and y-directions respectively in lower energy level for the silicon body orientation of (100), E_0 are the lowest subband energy. Values of the kinetic and potential energies are respectively written as

$$\begin{aligned} E_{0(kin)} &= \frac{\hbar^2}{2}\left(\int_0^H \frac{1}{m_x}\psi_0\frac{d^2\psi_0}{dx^2} + \int_0^W \frac{1}{m_y}\psi_0\frac{d^2\psi_0}{dy^2}\right) \\ E_{0(pot)} &= -q\int_0^W\int_0^H \psi_0\phi(x, y)\psi_0 dxdy \end{aligned} \tag{8}$$

From (6), the value of the lowest subband total energy is calculated to be,

$$E_0 = \langle E_{0(kin)}\rangle + \langle E_{0(pot)}\rangle \tag{9}$$

In the quantum variational approach, b_0 is evaluated by minimizing E_0, i.e., $dE_0/db_0 = 0$.

A good approximation for b_0 is derived as,

$$b_0 \approx (W + H)\pi^2\left(\frac{5}{12}\frac{q(m_x + m_y)Q_{inv}}{\varepsilon_{si}h^2}\right) \tag{10}$$

Note that the variational parameter (b_0) is dependent on the inversion charge density (Q_{inv}) and device dimensions (W and H).

In the classical case, the carrier density does reach its maximum at the Si-SiO_2 interface for all values of Vgs. In quantum mechanical case, the electrons are distributed more toward the center of silicon body and it has some influence in Vgs. Fig. 2 shows the plot of wave function in x direction for various values of gate voltage. It can be clearly seen that the electrons are spread throughout the silicon body and get

$$\phi(x, y) = \frac{\begin{pmatrix} e^{-(\alpha+\beta+\gamma)} \\ a_0b_0Q_{inv} \\ H^2W^2\pi^2 \end{pmatrix}\begin{bmatrix} e^{(\alpha+\beta)}\left(b_0H^4\cos\left(\frac{\pi x}{W}\right) + a_0W^4\pi^4\sin\left(\frac{\pi x}{W}\right)\right) \\ +H^2W^2\pi^2e^{(\beta+\gamma)}\left(b_0^3\cos\left(\frac{\pi(Hx-2Wy)}{HW}\right) + a_0^3\sin\left(\frac{\pi(Hx-2Wy)}{HW}\right)\right) \\ +e^{(\alpha+\gamma)}\left(b_0^5W^4\pi^4\cos\left(\frac{\pi(Hx+2Wy)}{HW}\right) + a_0^5H^4\sin\left(\frac{\pi(Hx+2Wy)}{HW}\right)\right) \end{bmatrix}}{4\varepsilon_{si}\omega\left(4b_0^2H^2 + \omega - 8b_0^2HW\right)\left(4b_0^2H^2 + \omega + 8b_0^2HW\right)(\omega + \delta)\left(4b_0^2H^2 + \omega + \delta - 8b_0^2HW\right)} \tag{6}$$

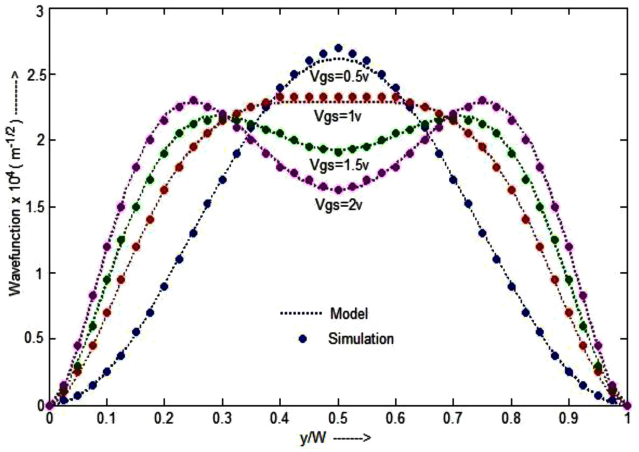

Fig. 2. The plot of probability density function versus normalized position of silicon film in y direction for various values of gate voltage (Vgs = 0.5 V, 1 V, 1.5 V and 2 V) and x = 1 nm. Dotted lines correspond to our model and symbols correspond to simulation data's.

their maximum value at different points within the silicon body depending on the gate voltage. For large value of Vgs the two electron density maxima related to each Si-SiO_2 interface. For small value of Vgs, these two maxima are merging. Fig. 3 shows the Inversion charge distribution function in x direction for different points in y direction at gate voltage of 0.5 V. The probability of inversion charge density is linearly increases with increasing y value. The model data's are well agreed (almost exactly) with those of simulation data's.

III. Parameters Modeling of Trigate MOSFETs

In the previous section, we found the inversion charge distribution function for trigate MOSFETs. This function is used to develop the analytical model for device parameters like centroid, inversion charge sheet density, threshold voltage, drain current and gate capacitance. In this section, we can develop an analytical model for the above parameters of trigate MOSFETs which includes the quantum effects.

In the classical case, the density maximum is always located directly at the interface. But in the quantum mechanical case, the electrons are distributed more toward the center of the silicon body. The expression for inversion charge density is given as [19],

$$Q_{inv} = 3C_{ox1}(V_{gs} - V_T) \tag{11}$$

where

$$C_{ox1} = \frac{C_{ox}}{1 + \left(\frac{\varepsilon_{ox}}{\varepsilon_{si}}\right)\left(\frac{x_I}{T_{ox}}\right)} \tag{12}$$

$$V_T = \phi_{ms} + \phi_{dep} + \frac{Q_D}{C_{ox}} \tag{13}$$

C_{ox} is the gate oxide capacitance. Based on [20], the classical oxide capacitance has been replaced as the series connection of oxide layer capacitance and semiconductor capacitance. Equation (12) and (13) can be replaced as,

$$C_{ox1} = \frac{C_{Total}}{1 + \left(\frac{\varepsilon_{ox}}{\varepsilon_{si}}\right)\left(\frac{x_I}{T_{ox}}\right)} \tag{14}$$

$$V_T = \phi_{ms} + \phi_{dep} + \frac{Q_D}{C_{Total}} \tag{15}$$

The total capacitance C_{Total} is given as

$$\frac{1}{C_{Total}} = \frac{1}{C_{oxide}} + \frac{1}{C_{Semiconductor}} \tag{16}$$

V_T is a constant threshold voltage for strong inversion, ϕ_{ms} is the work function difference between gate and silicon film and ϕ_{dep} is the depletion potential is given as,

$$\phi_{dep} = \phi_s - \frac{x_I Q_{inv}}{\varepsilon_{si}} \tag{17}$$

where, ϕ_s is the surface potential, x_I is the inversion charge centroid which is known as the average inversion layer penetration. It is the most interesting parameter to model and it has been used to quantify the influence of quantum effects on the inversion charge of MOS devices.The quantum charge distribution function is used to calculate the inversion charge centroid. The centroid x_I is obtained as,

$$x_I = \int_0^W \int_0^H xy\psi_0(x, y)dxdy$$

The final expression for x_I is given as,

$$x_I = \frac{\left\{\begin{array}{l} -4a_0^2 e^{-2b_0} H^3 \pi W^2 \left(\begin{array}{l} 4b_0^2 + \pi^2 \\ +\pi^2 \cosh(b_0) \end{array}\right) \\ \left[\begin{array}{l} b_0(b_0^2 + \pi^2)\cosh(b_0) \\ -\left(b_0^2(3 + b_0) + (1 + b_0)\pi^2 \sinh(b_0)\right) \end{array}\right] \end{array}\right\}}{b_0^2 HW(b_0^2 + \pi^2)^2(4b_0^2 + \pi^2)} \tag{18}$$

The centroid is validated for various values of silicon thickness, silicon width and inversion charge density N_{inv}.

The drain current of trigate MOSFETs can be obtained from the integration of inversion charge density in (11). The drain current in trigate MOSFET with the assumption that the mobility is independent of the position in the channel is expressed as,

$$I_d = \mu\pi\left(\frac{H + W}{L}\right)\int_0^{V_{ds}} Q_{inv}dV \tag{19}$$

$$I_{ds} = \frac{2\mu\pi(H + W)C_{ox1}}{L}\left[V_{gs}V_{ds} - \frac{V_{ds}^2}{2} - \phi_{ms}V_{ds} + A\left(\begin{array}{l} V_{gs}^2 V_{ds} - V_{gs}V_{ds}^2 - \frac{V_{ds}^3}{3} \\ -B\left(V_{gs}V_{ds} + \frac{V_{ds}^2}{2}\right) \end{array}\right) + 2V_{th}V_{ds}\left(\frac{Q_{inv}}{\varepsilon_{si}}\right)\right] \tag{20}$$

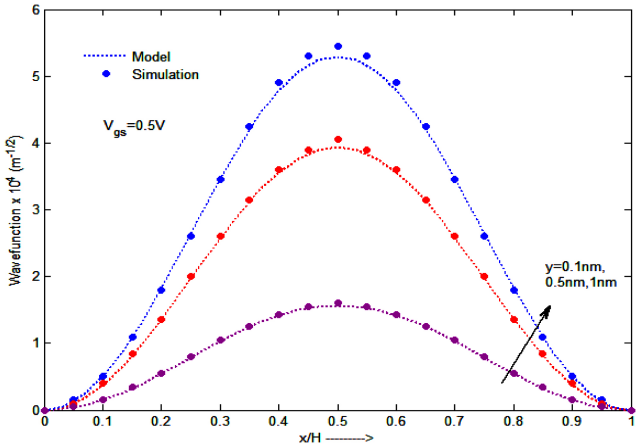

Fig. 3. Inversion charge distribution function plot for trigate MOSFET along x-axis for different values of y-values at Vgs = 0.5 v. Dotted lines correspond to our model and symbols correspond to simulation data's.

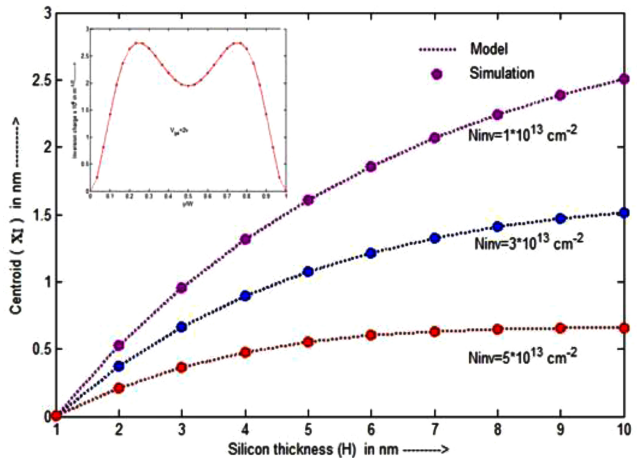

Fig. 4. Inversion charge centroids versus silicon thickness in trigate MOSFETs structure for various values of inversion electron concentration. Dotted lines correspond to our model and symbols correspond to simulation data's. (Inset) Simulation and analytical model derived inversion charge profile versus depth.

The final expression for drain current is given in (20). where, A and B are the closed form functions of α, β, γ, ω and δ given as,

$$A = \frac{e^{b_0}\left(b_0^3 + a_0\pi^3\right)}{\omega\left(4b_0^2H^2 + \omega + \delta - 8b_0^2HW\right)(\omega + \delta)}$$
$$B = 2a_0^2(\omega + \delta)\left(b_0^3 + b_0\pi^2\right) + \pi^2 e^{-b_0} \quad (21)$$

IV. Results and Discussion

The accuracy of the proposed model is verified using the commercially available TCAD Sentaurus device simulator. Sentaurus Device implements four different quantization models, such as Van Dort model, 1D Schrö dinger equation model, Density gradient model and Modified local-density approximation (MLDA) model. In our work the 1D Schrö dinger equation model is used to evaluate the influence of quantization effects.

Fig. 4 shows that, inversion charge centroid (x_I) in (19) versus silicon thickness (H) for different values of inversion

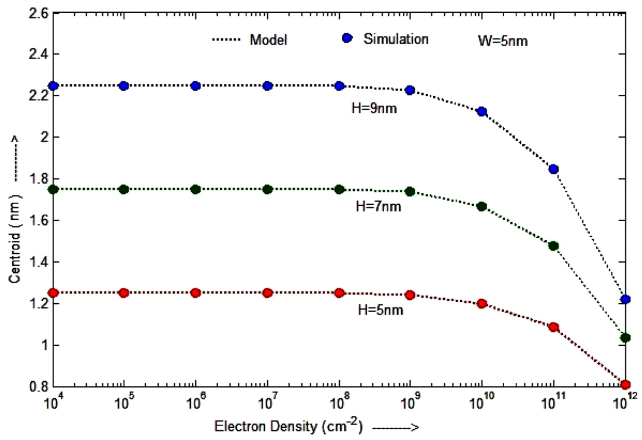

Fig. 5. Inversion charge centroid versus electron density for trigate MOSFETs at room temperature with $H = 5$, 7 and 9 nm and $W = 5$ nm. The simulation results obtained, including quantization, are plotted in symbols. The data obtained making use of the model is plotted in dotted lines.

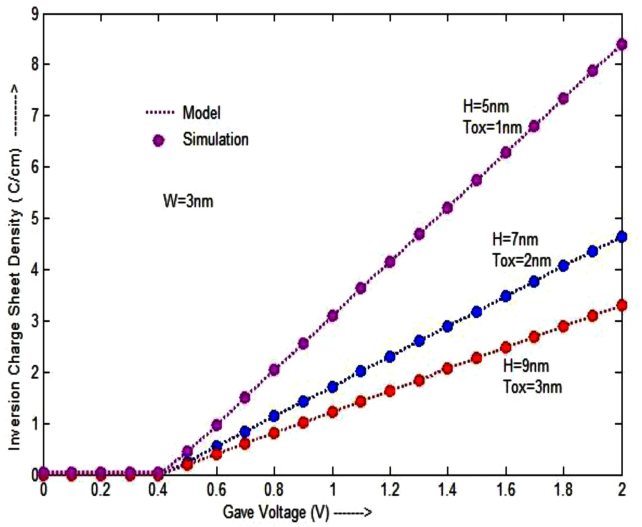

Fig. 6. Inversion charge density in trigate MOS structures as a function of the gate voltage. Three sets of trigate SOI MOSFETs are considered with $W = 3$ nm. (Dotted line) Our model is compared with (symbols) simulation results.

charge density (N_{inv}). For relatively high thickness, the inversion charge centroid x_I decreases with increasing N_{inv} due to the high electric field at the Si/SiO_2 interface caused by quantum effects. For the small thickness regime, the charge centroid depth with respect to the gate interface in fact increases linearly with Si thickness and depends on N_{inv}. The inversion charge centroid can account for the oxide interface separation of the inversion charge distribution.

We calculated the inversion charge centroid making use of our model the results versus inversion charge density (N_{inv}) are plotted in Fig. 5. The centroid shows the expected behavior and it can be seen that its value decreases as the inversion charge increases since the charge distribution shifts toward the Si/SiO_2 interface. The model presented here exactly matches with simulation data's for different silicon thickness.

The inversion charge density in quantum model is always smaller than classical model because of energy quantization.

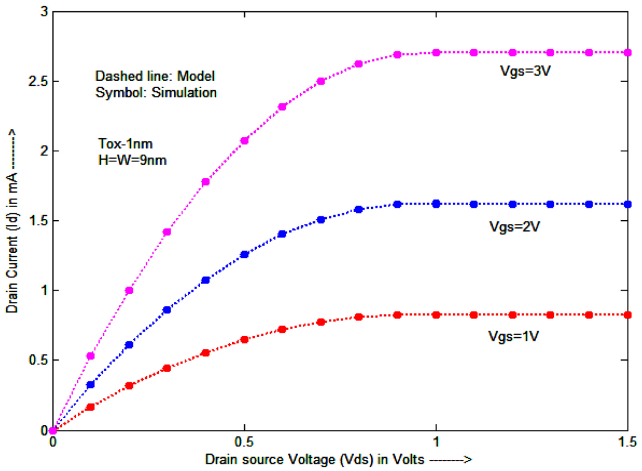

Fig. 7. Drain current versus drain source voltage in trigate MOSFETs with various values of gate voltages. Dashed line: our model using (20). Symbols: simulation.

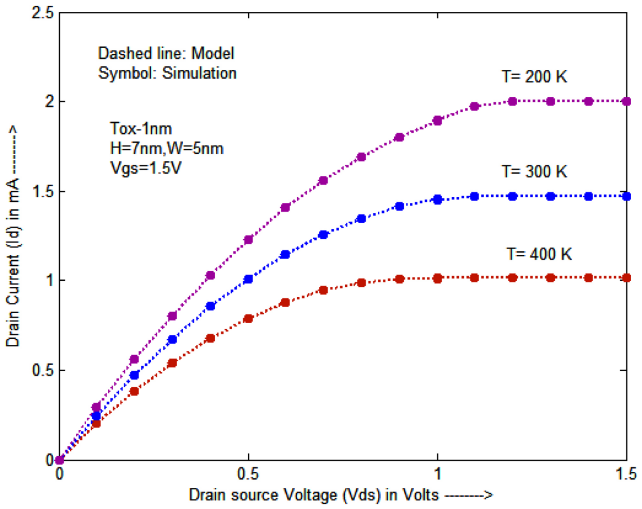

Fig. 8. Drain current versus drain source voltage with various temperature (T) for trigate MOSFETs.

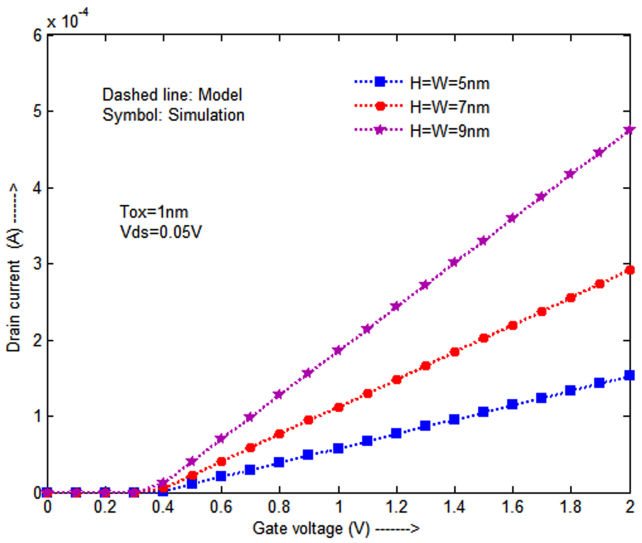

Fig. 9. Drain current versus gate voltage in trigate MOSFETs at Vds = 0.05V with different device dimensions. Dashed line: our model using (20). Symbols: simulation.

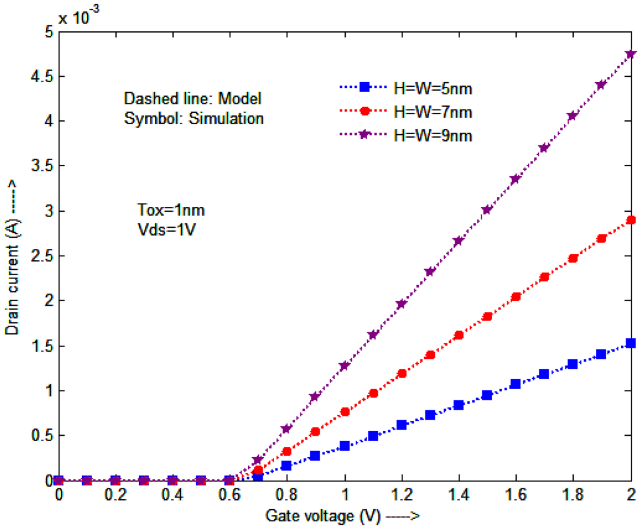

Fig. 10. Drain current versus gate voltage in trigate MOSFETs at Vds = 1V with different device dimensions. Dashed line: our model using (20). Symbols: simulation.

Fig. 6 represents the plot of total inversion charge with the gate voltage for various values of silicon thickness and gate oxide. From the figure we can observe that, the inversion charge density increases above threshold voltage for all device dimensions. It also shows that, the inversion charge density linearly increases for smaller device dimensions. The single analytical expression (11) is used for all the three regions of device operation.

Fig. 7 shows the drain current versus drain voltage characteristics of trigate MOSFETs for different values of gate voltages (Vgs). From the figure, we can observe that the drain current differences increase with increasing gate voltage and/or drain voltage. The drain current increases linearly for small dimensions of device when compare with larger dimensions. Very good agreement is obtained between the simulation and the analytical model.

The change in drain current of TG MOSFET with temperature are shown in Fig. 8 and compared with simulation data's. From the figure, it is observed that, the drain current is increased at low temperatures. The influence of temperature in drain current will dominate at higher drain to source voltages. Fig. 9 and Fig. 10 shows the $I_d - V_{gs}$ characteristics obtained from the model using Eq. (20) for $V_{ds} = 0.1$ V and $V_{ds} = 1.0$ V respectively. Also the results are compared with the simulated data. The saturation region and the linear region

$I_d - V_{gs}$ curves are considered in these figures and they are important for device design. For linear region $I_d - V_{gs}$ plot is shown in fig. 9 and the value of V_{ds} is 0.05 V and for saturation region the $I_d - V_{gs}$ plot is shown in fig. 10 where the V_{ds} value is 1 V. Fig. 11 shows a typical curve of drain current (I_d) versus gate voltage (V_{gs}) in logarithmic scale. It allows measurement of many device parameters such as threshold voltage, and the slop of V_{gs} versus Ids in weak inversion state. From the figure we find the transistor off-state

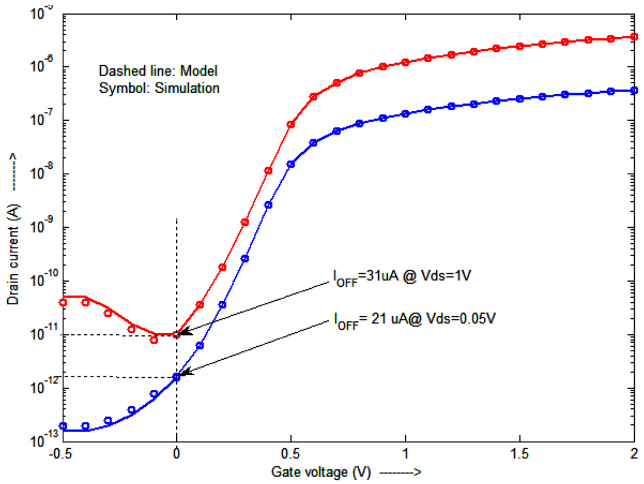

Fig. 11. Log (I_d) Versus Vgs for Tri-Gate MOSFETs for different drain Voltages. (Dotted line) Our model is compared with (symbols) simulation results.

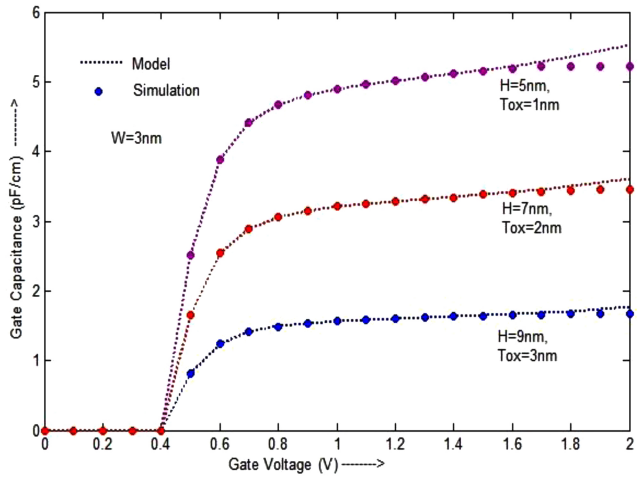

Fig. 12. Gate capacitance of trigate MOS structure as a function of the gate voltage with various cross sections and $W = 3$ nm. (Dotted line) Our model is compared with (symbols) simulation results.

current, which is the drain current when the gate voltage is zero. The Tri-gate transistor has an I_{OFF} of 31 μA and 21 μA at the drain voltage of 1 V and 0.05 V, respectively shown in figure. In quantum case, the inversion charge centroid is farther away from the interface, as compared with that of the classical approach. This results in the variation of gate capacitance C_g when we include the quantum effects. So, it is important to calculate the gate capacitance value. The gate capacitance of a trigate MOSFET may be obtained from dQ_{inv}/dV_{gs}. The gate capacitance value well captured by our model is shown in Fig. 12 and compared with the simulation data's. As shown in figure, quite a good fit is achieved in both the weak and strong inversion regions.

V. Conclusion

We have developed an analytical model for trigate MOSFETs including quantum effects. By introducing an inversion charge distribution function for trigate MOSFETs, a simple and accurate quantum analytical model is proposed and demonstrated using variational approach. This compact model becomes explicit by using inversion charge density expression in terms of gate voltage. Good agreement is found between our analytical quantum data's and simulation data's for different device dimensions and applied voltages.

Acknowledgment

The authors would like to thank Prof. D. Misra and Mr. S. T. Chandra for the helpful discussion.

References

[1] D. J. Frank, R. H. Dennard, E. Nowak, P. M. Solomon, Y. Taur, and H.-S. P. Wong, "Device scaling limits of Si MOSFETs and their application dependencies," *Proc. IEEE*, vol. 89, no. 3, pp. 259–288, Mar. 2001.

[2] B. Doyle, R. Arghavani, D. Barlage, S. Datta, M. Doczy, J. Kavalieros, *et al.*, "Transistor elements for 30 nm physical gate lengths and beyond," *Intel Technol. J.*, vol. 6, no. 2, pp. 42–54, May 2002.

[3] J. He, F. Liu, W. Bian, J. Feng, J. Zhang, and X. Zhang, "An approximate carrier-based compact model for fully depleted surrounding-gate MOSFETs with a finite doping body," *Semicond. Sci. Technol.*, vol. 22, no. 6, pp. 671–677, Jun. 2007.

[4] A. Son, J. Kim, N. Jeong, J. Choi, and H. Shin, "Improved explicit current-voltage model for long-channel undoped surrounding-gate metal oxide semiconductor field effect transistor," *J. Appl. Phys.*, vol. 48, pp. 412–413, Apr. 2009.

[5] Y. Chen and J. Luo, "A comparative study of double-gate and surrounding-gate MOSFETs in strong inversion and accumulation using an analytical model," in *Proc. Int. Conf. Model. Simulation Microsyst.*, vol.1. 2001, pp. 546–549.

[6] D. Jimenez and B. Inguiez, "Continuous analytic IV model for surrounding-gate MOSFETs," *IEEE Electron Device Lett.*, vol. 25, no. 8, pp. 571–573, Aug. 2004.

[7] B. Iniguez, D. Jimenez, J. Roig, H.-A. Hamidi, L. F. Marsal, and J. Pallares, "Explicit continuous model for long-channel undoped surrounding-gate MOSFETs," *IEEE Trans. Electron. Devices*, vol. 52, no. 8, pp. 1868–1873, Aug. 2005.

[8] J. P. Colinge, *FinFETs and Other Multi-Gate MOSFETs*. Berlin, Germany: Springer, 2008.

[9] A. Kranti and G. A. Armstrong, "Performance assessment of nanoscale double-and triple-gate FinFETs," *Semicond. Sci Technol.*, vol. 21, no. 2, pp. 409–421, Apr. 2006.

[10] Y. W. Jin, C. Zeng, L. Ma, and D. Barlage, "Analytical threshold voltage model with TCAD simulation verification for design and evalution of tri-gate MOSFETs," *Solid State Electron.*, vol. 51, pp. 347–353, Mar. 2007.

[11] A. Tsormpatzoglou, C. A. Dimitriadis, R. Clerc, G. Pananakakis, and G. Ghibaudo, "Semianalytical modeling of short-channel effects in lightly doped silicon trigate MOSFETs," *IEEE Trans. Electron. Devices*, vol. 55, no. 10, pp. 2623–31, Oct. 2008.

[12] A. Tsormpatzoglou, D. H. Tassis, C. A. Dimitriadis, G. Ghibaudo, N. Collaert, and G. Panankakis, "Analytical threshold voltage model for lightly doped short-channel tri-gare MOSFETs," *Solid State Electron.*, vol. 57, pp. 31–34, Mar. 2011.

[13] J. G. Fossum, L. Ge, M. H. Chiang, V. P. Trivedi, M. M. Chowdhury, L. Mathew, *et al.*, "A process/physics-based compact model for nonclassical CMOS device and circuit design," *Solid State Electron.*, vol. 48, no. 6, pp. 919–926, Jun. 2004.

[14] P. Vimala and N. B. Balamurugan, "Modeling the centroid and inversion charge density in double-gate MOSFETs including quantum effects," *Int. J. Electron.*, vol. 100, no. 9, pp. 1283–95, Sep. 2013.

[15] P. Vimala and N. B. Balamurugan, "Analytical modeling of quantization effects in surrounding-gate MOSFETs," *COMPEL Int. J. Comput. Math. Electr. Electron. Eng.*, vol. 33, nos.1–2, 2014, to be published.

[16] J.-P. Colinge, J. C. Alderman, W. Xiong, and C. R. Cleavelin, "Quantum Mechanical effects in trigate SOI MOSFET," *IEEE Trans. Electron Devices*, vol. 53, no. 5, pp. 1131–1136, May 2006.

[17] R. Granzner, S. Thiele, C. Schippel, and F. Schwierz, "Quantum effects on the gate capacitance of trigate SOI MOSFETs," *IEEE Trans. Electron Devices*, vol. 57, no. 12, pp. 3231–3238, Dec. 2010.

[18] P. R. Kumar and S. Mahapatra, "Analytical modeling of quantum threshold voltage for triple gate MOSFET," *Solid State Electron*, vol. 54, pp. 1586–1591, Aug. 2010.
[19] E. Moreno, J. B. Roldan, F. G. Ruiz, D. Barrera, A. Godoy, and F. Gamiz, "An analytical model for square GAA MOSFETs including quantum effects," *Solid State Electron*., vol. 54, pp. 1463–1469, Jul. 2010.
[20] J. A. López-Villanueva, P. Cartujo-Casinello, J. Banqueri, F. Gámiz, and S. Rodríguez, "Effects of the inversion layer centroid on MOSFET behaviour," *IEEE Trans. Electron. Devices*, vol. 44, no. 11, pp. 1915–1922, Nov. 1997.
[21] J. B. Roldan, A. Godoy, F. Gamiz, and M. Balaguer, "Modeling the centroid and the inversion charge in cylindrical surrounding gate MOSFETs, including quantum effects," *IEEE Trans. Electron. Devices*, vol. 55, no. 1, pp. 411–416, Jan. 2008.

P. Vimala received the B.E. and M.E. degrees both in electronics and communication engineering from Anna University, Chennai, Tamil Nadu, India. She is currently pursuing the Ph.D. degree with the Department of Electronics and Communication Engineering, Thiagarajar College of Engineering, Tamil Nadu, under Anna University. She is awarded with the Women Scientist Fellowship for three years for her research work from the Department of Science and Technology, Government of India, Delhi, India. Her current research interests include quantum modeling and simulation of multigate MOSFETs. She is currently engaged in the modeling of energy quantization in tri-gate MOSFETs and analyzing its performance using the Synopsis TCAD Simulation tool.

N. B. Balamurugan received the B.E. and M.E. degrees both in electronics and communication engineering from the Thiagarajar College of Engineering (TCE), Tamil Nadu, India. He received the Ph.D. degree in nanoelectronics from Anna University, Chennai, Tamil Nadu, India. From 1998 to 2004, he was a lecturer with the R.V.S. College of Engineering and Technology, Tamil Nadu. He is currently an Assistant Professor with the Department of Electronics and Communication Engineering, TCE. He has published over 50 research papers as a sole or joint author in the field of device modeling and simulation. His current research interests include analytical modeling and simulation of semiconductor device structures, such as nanoscale SOI MOSFETs, nanowire transistors tunnel FET, quantum effects in multigate MOSFETs, and design and simulation of VLSI fuzzy processing.